Global ocean heat content over the past 3 million years

Sarah Shackleton

sarah.shackleton@whoi.edu

Woods Hole Oceanographic Institution https://orcid.org/0000-0001-5927-1954

Valens Hishamunda

Princeton University https://orcid.org/0000-0003-1043-6847

Yuzhen Yan

Tongji University

Austin Carter

University of California at San Diego

Jacob Morgan

University of California at San Diego

Jeffrey Severinghaus

Scripps Institution of Oceanography

Sarah Aarons

Scripps

Julia Marks Peterson

Oregon State University

Jenna Epifanio

Oregon State University

Christo Buizert

Oregon State University https://orcid.org/0000-0002-2227-1747

Ed Brook

Oregon State University

Andrei Kurbatov

University of Maine System https://orcid.org/0000-0002-9819-9251

Mike Bender

Princeton University

John Higgins

Princeton University https://orcid.org/0000-0002-4893-4561

Physical Sciences - Article

Keywords:

Posted Date: January 6th, 2025

DOI: https://doi.org/10.21203/rs.3.rs-5610580/v1

Additional Declarations: There is **NO** Competing Interest.

Version of Record: A version of this preprint was published at Nature on March 18th, 2026. See the published version at https://doi.org/10.1038/s41586-026-10116-3.

Abstract

The Pleistocene Epoch is characterized by global cooling and an increase in the intensity and duration of glacial cycles. Regional surface and subsurface ocean temperature records follow distinct trends over this interval, suggesting dynamic changes in zonal and meridional heat transport and ocean circulation. Here we provide a record of global ocean heat content (or mean ocean temperature) over the last 3 million years from ice core noble gas (Xe/Kr) measurements. We find long-term ocean cooling over this interval, a prominent period of cooling coincident with the Plio-Pleistocene transition (~2.7 Ma), and steady temperatures across the mid-Pleistocene transition (1.2-0.8 Ma). Comparisons with a recent global sea surface temperature compilation show broad consistency in long-term cooling, but important differences at the Plio-Pleistocene and mid-Pleistocene transitions. We suggest that the different trends in surface temperature and mean ocean temperature during these intervals are related to a redistribution of heat between the surface and subsurface via changes in deep water formation and upwelling. Our temperature record also permits an estimate of global ice volume changes between 3 and 0.5 Ma through a deconvolution of the benthic foraminiferal δ18O record pointing to a period of enhanced ice sheet growth around the mid-Pleistocene transition.

Full Text

The last 3 million years of Earth's climate history are punctuated by two important events, 1) the onset of large-scale Northern Hemisphere glaciation and strengthening of the 41-kyr periodicity in glacial cycles at the Plio-Pleistocene transition (PPT; 2.7 Ma) and 2) the shift in periodicity from 41kyr to 100kyr periodicity at the Mid-Pleistocene Transition (MPT; 1.2 to 0.8 Ma). Critically, the paleoclimate record that best characterizes these two key events - the oxygen isotopic composition (δ^{18}O) of benthic foraminifera - is a somewhat ambiguous metric of Earth's climate system as it tracks both the size of the ice sheets and the temperature of the oceans[1,2]. Consequently, the global expression and driving mechanisms of the PPT and MPT remain subjects of ongoing debate.

Measurements of noble gases in air trapped in ice cores (Xe/Kr) provide a direct constraint on global ocean temperature through the temperature-dependent solubilities of these gases[3]. Variations in atmospheric Xe/Kr are driven by the changes in the fraction of these gases dissolved in the oceans, which is primarily controlled by mean ocean temperature (MOT) change. Because the temperature dependence of xenon's solubility is greater than that of krypton, a change in ocean temperature leads to a larger change in the ocean/atmosphere partitioning of xenon relative to krypton; whole ocean cooling leads to a decrease in atmospheric Xe/Kr and warming leads to an increase.

Here we report noble gas measurements in new Allan Hills ice core archives to examine ocean temperature evolution over the last 3 million years. Noble gas-based MOT provides a precise estimate of the global ocean heat, a quantity that reflects both global radiative forcing and the distribution of heat through circulation. When combined with reconstructions of local/regional temperatures from marine-based proxies, MOT provides a critical boundary condition that constrains plausible changes in radiative

forcing and ocean vertical mixing. Here we report, for the first time, a noble gas-based MOT record spanning the last 3 million years from measurements in new ice core archives from Allan Hills[4].

3 million year old ice core reconstruction of Mean Ocean Temperature

We present measurements from three shallow (~200 meter) Allan Hills ice cores drilled in the 2019-2020 and 2022-2023 field seasons. Two ice cores (ALHIC1901 and ALHIC1902, figure S1) come from a region within the Allan Hills blue ice field where horizontal and vertical velocities approach zero[5] and are located near previously drilled ice cores that contain stratigraphically disordered ice older than 2 million years[6]. The third ice core (ALHIC1903) contains a continuous record spanning the Penultimate Glacial Maximum and Last Interglacial ((~115-150 ka[7,8]). Samples from this core preserve the full range of glacial-interglacial variability from the Allan Hills blue ice area, which we use for comparison when evaluating older climate 'snapshots' from ALHIC1901 and ALHIC1902 that are not in stratigraphic order. In addition, we include published argon isotope and Xe/Kr measurements from ALHIC1502 and ALHIC1503 in our MOT analysis[6].

MOT reconstructions from Allan Hills ice core records covering Termination II and the Last Interglacial match published records in range[9] (Figure S2), but indicate a consistent cold bias of up to 0.5°C in the Allan Hills MOT reconstruction relative to published values. This aligns with other studies showing reconstructions of MOT change are more reliable than absolute MOT values[9–11]. To account for this, relative and absolute MOT uncertainties are reported (Methods).

Sample dating relies on the contemporary ^{40}Ar degassing rate and measured ^{40}Ar deficit relative to the modern atmosphere (and corrected for gravitational enrichment, $\delta^{40}Ar_{atm}$)[12]. Uncertainties in dating arise from analytical precision in $\delta^{40}Ar_{atm}$ measurements and ^{40}Ar degassing rates, with larger absolute uncertainties in older samples due to the 11% uncertainty in ^{40}Ar degassing. The deepest dated samples in ALHIC1901 and ALHIC1902 extend back to 4.0±0.4 Ma and 6.0±0.7 Ma, respectively—significantly older than previously dated ice from this region[4].

The ALHIC1901 dating illustrates a complex stratigraphy, with multiple age reversals and large age variations over narrow depth windows (Figure S1). In the most extreme case, at ~148 meters depth, we find a ~2-million-year age change over less than a meter. Such variation is likely also present in the ALHIC1502 and ALHIC1503 cores, but these cores were not dated at sufficiently high depth resolution to assess the full extent of stratigraphic disturbance. The abrupt variations in age with depth argue against strong signal attenuation. As in refs [4] and [13], we consider the possibility for a depth dependence in the resolution of these snapshots. Following this convention, the samples are characterized into short-exposure snapshots that preserve some/most/all of the true glacial-interglacial variability, and long-exposure snapshots that preserve climate signals that more closely represent the mean over glacial cycles. The short-exposure snapshots are limited to samples <900 ka, and therefore, their inclusion or exclusion in our analysis has no influence on the long-term trends suggested by the data.

Figure 1 shows reconstructed MOT for the Allan Hills samples. We find evidence - in the form of implausible Xe/Kr/Ar ratios - for noble gas alteration in the deepest, oldest parts of each core (see methods), limiting our MOT reconstruction to the last 3.1 Ma. Our record reveals a 2 ± 0.4°C cooling between the late Pliocene (~3 Ma) and the onset of the MPT at 1.2 Ma. Although gaps exist, much of this cooling seems to coincide with Northern Hemisphere glaciation intensification at the PPT (~2.7 Ma). Importantly, no significant MOT trends are observed across the MPT.

Ocean heat content changes

Ice core-based MOT offers unique new constraints for resolving global ocean temperature changes over the last 3 million years. While global benthic foraminifera δ^{18}O compilations contain information about deep ocean temperature, the ice volume effect is comparable in magnitude and difficult to separate out. Deep ocean temperature (DOT) reconstructions for the Pleistocene are limited to several Mg/Ca-based records and show significant inter-basin differences during key intervals of this period[14]. The new Allan Hills Xe/Kr record provides a global context for understanding these regional deep ocean temperature trends.

Only one high-resolution Mg/Ca-based DOT reconstruction covers the PPT, a record from the North Atlantic[15]. This reconstruction suggests strong (~2°C) cooling across the PPT, consistent with—though approximately twice the magnitude of—the reconstructed MOT trend for this interval (Figure 2). We are not aware of records from other ocean basins for this period. However, reconstructions of the mid-Piacenzian (~3.3-3.0 Ma) in multiple ocean basins indicate warmer than present DOTs globally within this period, with a more substantial temperature anomaly in the Atlantic compared to other basins [16]. The differing inter-basin DOT anomalies for this period are broadly consistent with the larger magnitude of Atlantic DOT change compared to MOT across the PPT.

Reconstructed MOT shows no robust trend across the MPT (1.2-0.8 Ma). Several Mg/Ca-based DOT records exist for comparison[14,15,17]. While cooling is observed in the deep Atlantic[15]), the deep North [14] and South[17] Pacific show no cooling, or even slight warming across the MPT. The differing trends between ocean basins are key evidence for the complex dynamics at play; because MOT averaged over all depths and basins, it provides crucial context for the interpretation of available DOT records.

Surface-subsurface temperature decoupling

Next, we compare the MOT results to a recent global SST compilation and reconstruction of regional SST change[18]. We observe broad agreement in the overall global SST and MOT trends of long-term cooling across the Plio-Pleistocene. However, the records differ in detail; the global SST reconstruction shows a steady cooling from ~4 to 1.5 Ma, followed by accelerated cooling from 1.5 to 0.9 Ma, with the highest rates centered on the MPT. In contrast, the reconstructed MOT indicates accelerated cooling centered on the PPT and no cooling across the MPT. These observations suggest SST-MOT decoupling during both the PPT and MPT.

Surface and interior ocean temperatures are key climate parameters fundamentally linked to the global energy budget. Surface temperatures are influenced by shortwave and longwave radiation fluxes, zonal and meridional transport, and ocean-atmosphere heat exchange. Wind-driven and buoyancy-driven circulation changes related to upwelling, intermediate, and deep-water formation and ventilation control the distribution of heat between the surface and interior layers, and therefore the SST-MOT coupling. Below, we explore processes that may cause surface and subsurface temperatures to become decoupled, particularly in the context of global MOT and SST changes, and regional surface and subsurface trends across the PPT and MPT.

Enhanced subsurface cooling at the Plio-Pleistocene transition driven by intensification of Northern Hemisphere glaciation

What mechanisms may lead to an enhanced deep/mean ocean cooling without a prominent expression at the surface at the Plio-Pleistocene boundary? The PPT is marked by large-scale Northern Hemisphere glaciation. General circulation model (GCM) simulations by ref [19] suggest that Northern Hemisphere ice sheet growth was associated with only minimal sea surface temperature (SST) changes, but a significant shift in North Atlantic winter tropospheric circulation. This shift may have altered interior ocean properties via changes in wintertime deepwater formation, without requiring a strong global expression in SST.

Recent single forcing experiments with fully coupled GCMs, such as the TraCE-ICE experiment[20] offer new insight. In response to imposing a Laurentide Ice Sheet, these simulations show minimal surface temperature changes, but enhanced mean ocean cooling driven by increased wintertime deep convection. In addition to the strong MOT (relative to SST) response, the simulation suggests that North Atlantic DOT cooled about twice as much as MOT, broadly consistent with regional temperature reconstructions across the PPT (Figure 2a, Figure 3S).

Despite differences between TraCE-ICE (LGM) boundary conditions and those during the late Pliocene/early Pleistocene, model results appear to be robust across various climate states; Broccoli and Manabe's preindustrial-boundary simulations align with the TraCE-ICE findings though they lack subsurface data for validation. Additionally, although the LGM-Preindustrial ice sheet changes were likely larger than those at the PPT, the coupling between ocean heat content and ice extent in TraCE-ICE is strongest under intermediate/small ice sheet boundary conditions (Figure S3), suggesting that even small Northern Hemisphere ice sheets could impact deep/mean ocean temperatures. Future research should further investigate this ice sheet-ocean coupling and improve MOT resolution at the PPT to better constrain the timing and magnitude of ocean cooling.

Surface-interior decoupling across the mid-Pleistocene transition suggest change in the structure of vertical ocean heat fluxes

Ocean temperature reconstructions from the early Pleistocene suggest long term cooling of both the surface and interior, and an increase in both meridional temperature gradients and zonal temperature

gradients across the equatorial Pacific[18,21]. These trends are consistent with the gradual emergence of the eastern equatorial Pacific cold tongue, which may have played a key role in global surface cooling across this interval[21,22].

The MPT reflects a departure from this gradual trend; at its onset (~1.2 Ma), cooling of the eastern equatorial Pacific accelerates and then ceases by ~1Ma. At this time SST trends in the eastern and western equatorial Pacific converge (Figure 2c). This shift aligns with the strongest rates of global SST cooling in the past 4.5 million years and largest increase in SST variance[18]. In contrast, the noble gas-based reconstructions show no long-term MOT change across the MPT. We speculate that these contrasting trends are driven by the permanent establishment of the cold tongue, which represents a substantial fraction of the modern atmosphere-ocean heat flux and dominant source of interannual climate variability.

The establishment of the cold tongue provides a mechanism for substantial global surface cooling[22], while simultaneously increasing total ocean heat content through enhanced atmosphere-ocean heat exchange and strong tropical shortwave radiative forcing, effectively decoupling global SST and MOT. Part of this global surface cooling signal would have been transferred to the interior ocean through intermediate and deep-water formation sites (such as the North Atlantic), counterbalancing the ocean heat flux in the tropics in a manner consistent with observed SST, DOT, and MOT trends.

Ocean temperature / ice volume evolution across the Pleistocene

Noble gas-derived MOT provides a unique tool to disentangle the ocean temperature contribution to global benthic δ^{18}O records from changes in seawater δ^{18}O due to the changes in the volume and/or isotopic composition of polar ice sheets[23]. From 3 to 0.5 Ma, benthic δ^{18}O increased by approximately 0.95‰. Using our MOT reconstruction and the ref [24] paleotemperature equation, we estimate that ~70% of this increase (0.67‰) resulted from ocean cooling, while the remaining 0.28‰ reflects changes in seawater δ^{18}O driven by changes in the ice sheets (Figure 3).

The ~0.28‰ increase in the d^{18}O of seawater can be further broken down into contributions from an increase in the volume of the polar ice sheets and changes in the isotopic composition of the polar ice sheets. New direct measurements of the East Antarctic ice sheet in the Early Pleistocene[4] indicate a ~3-4‰ decline in δ^{18}O from 3.0 to 0.5 Ma. Assuming this decline is representative of global changes in the isotopic composition of ice sheets, this would account for about a quarter (0.07‰) of the 0.28‰ increase in the δ^{18}O of seawater. The remaining 0.21‰ would then be due to increased ice sheet volume and associated lowering of eustatic sea-level. Using an oxygen isotope mass balance model[25] and assuming the global ice volume increase is primarily driven by the development of ice sheets in the Northern Hemisphere, we estimate that a 0.28‰ increase in seawater δ^{18}O in combination with a 4‰ decline of the global ice sheets between 3.0 and 0.5 Ma would be associated with a ~24 meter lowering of sea-level over this interval (methods). Although a rigorous evaluation of the tempo of ice sheet growth

across the Pleistocene is beyond the scope of this study, we note that the largest period of ice sheet growth coincides with the MPT (Figure 3).

As an independent check on our seawater $\delta^{18}O$ estimate, we can compare it with records of the $\delta^{18}O$ of O_2 from the same Allan Hills ice cores[13]. The $\delta^{18}O$ of atmospheric O_2 is a complex tracer of photosynthesis and respiration in the marine and terrestrial biosphere that exhibits considerable variability on both orbital and millennial timescales[26–28] due to changes in the hydrological cycle at low latitudes and/or the isotopic fractionation associated with respiration, a set of processes collectively known as the Dole Effect[29]. As the ultimate source of H_2O for all photosynthesis, changes in the $\delta^{18}O$ of O_2 also reflect the changes in the $\delta^{18}O$ of seawater. Between 2.7 and 0.5 Ma, $\delta^{18}O$ of O_2 measured in Allan Hills ice core samples increased by ~0.3‰. This result is similar to, but slightly larger than, the 0.28‰ increase in seawater $\delta^{18}O$ between 3 to 0.5 Ma estimated from changes in MOT and the $\delta^{18}O$ values of benthic foraminifera.

Conclusions

The first direct noble gas record of MOT from recently discovered Pliocene and Pleistocene ice cores in the Allan Hills Blue Ice Area, East Antarctica, reveal a long-term cooling of 2-2.5 °C between 3 million years and the Late Pleistocene (0.5 Ma). Cooling appears to have been strongest around the PPT with little (if any) MOT cooling occurring across the MPT (Figure 1). Greenhouse gas data from the same Allan Hills ice cores show a ~25 ppm CO_2 decrease and minimal change in CH_4 across the early Pleistocene[13] (2.7 to 1.2 Ma), suggesting that cooling is accompanied by a relatively modest decline in atmospheric greenhouse gas concentrations. The decoupling of MOT and SST trends throughout the Pleistocene, likely driven by ice sheet dynamics and shifts in ocean circulation and mixing, support this observation, suggesting that factors other than direct radiative forcing from greenhouse gases likely explain most of the ocean cooling we observe over the Plio-Pleistocene. Future research into the interactions among ice sheets, ocean circulation, the terrestrial biosphere, and the global energy budget will be essential in providing a clearer picture of climate evolution over the Plio-Pleistocene.

References

1. Shackleton, N. Oxygen isotope analyses and pleistocene temperatures re-assessed. Nature 215, 15–17 (1967).
2. Emiliani, C. Pleistocene Temperatures. J. Geol. 63, 538–578 (1955).
3. Headly, M. A. & Severinghaus, J. P. A method to measure Kr/N 2 ratios in air bubbles trapped in ice cores and its application in reconstructing past mean ocean temperature. J. Geophys. Res. 112, D19105 (2007).
4. Shackleton, S. et al. 6 million-year-old ice and air from the Allan Hills blue ice area, East Antarctica. Submitted (2024).

5. Spaulding, N. E. et al. Ice motion and mass balance at the Allan Hills blue-ice area, Antarctica, with implications for paleoclimate reconstructions. J. Glaciol. 58, 399–406 (2012).
6. Yan, Y. et al. Two-million-year-old snapshots of atmospheric gases from Antarctic ice. Nature 574, 663–666 (2019).
7. Carter, A. et al. Evidence for diminished Ross Ice Shelf and West Antarctic Ice Sheet during the Last Interglacial from ice cores at the Allan Hills, Antarctica. Submitted (2024).
8. Spaulding, N. E. et al. Climate archives from 90 to 250 ka in horizontal and vertical ice cores from the Allan Hills Blue Ice Area, Antarctica. Quat. Res. 80, 562–574 (2013).
9. Shackleton, S. et al. Global ocean heat content in the Last Interglacial. Nat. Geosci. 13, 77–81 (2020).
10. Baggenstos, D. et al. Earth's radiative imbalance from the Last Glacial Maximum to the present. Proc. Natl. Acad. Sci. U. S. A. 116, 14881–14886 (2019).
11. Haeberli, M. et al. Snapshots of mean ocean temperature over the last 700 000 years using noble gases in the EPICA Dome C ice core. Clim. Past 17, 843–867 (2021).
12. Bender, M. L., Barnett, B., Dreyfus, G., Jouzel, J. & Porcelli, D. The contemporary degassing rate of 40Ar from the solid Earth. Proc. Natl. Acad. Sci. U. S. A. 105, 8232–8237 (2008).
13. Marks Peterson, J. et al. Stable Pleistocene atmospheric CO2 and CH4 levels from ice cores from the Allan Hills, Antarctica. Submitted (2024).
14. Ford, H. L. & Raymo, M. E. Regional and global signals in seawater δ18O records across the mid-Pleistocene transition. Geology 48, 113–117 (2020).
15. Sosdian, S. & Rosenthal, Y. Deep-Sea Temperature and Ice Volume Changes Across the Pliocene-Pleistocene Climate Transitions. Science (80-.). 325, 306–310 (2009).
16. Dowsett, H. J., Robinson, M. M. & Foley, K. M. Pliocene three-dimensional global ocean temperature reconstruction. Clim. Past 5, 769–783 (2009).
17. Elderfield, H. et al. Evolution of ocean temperature and ice volume through the mid-Pleistocene climate transition. Science (80-.). 337, 704–709 (2012).
18. Clark, P. U., Shakun, J. D., Rosenthal, Y., Köhler, P. & Bartlein, P. J. Global and regional temperature change over the past 4.5 million years. Science (80-.). 383, 884–890 (2024).
19. Broccoli, A. J. & Manabe, S. The influence of continental ice, atmospheric CO2, and land albedo on the climate of the last glacial maximum. Clim. Dyn. 1, 87–99 (1987).
20. Liu, Z. et al. Transient Simulation of Last Deglaciation with a New Mechanism for Bølling-Allerød Warming. Science (80-.). 325, 310–314 (2009).
21. Martínez-Garcia, A., Rosell-Melé, A., McClymont, E. L., Gersonde, R. & Haug, G. H. Subpolar Link to the Emergence of the Modern Equatorial Pacific Cold Tongue. Science (80-.). 328, 1550–1553 (2010).
22. Philander, S. G. & Fedorov, A. V. Role of tropics in changing the response to Milankovich forcing some three million years ago. Paleoceanography 18, (2003).

23. Shackleton, S., Seltzer, A., Baggenstos, D. & Lisiecki, L. E. Benthic δ18O records Earth's energy imbalance. Nat. Geosci. 16, 797–802 (2023).
24. Shackleton, N. J. Attainment of isotopic equilibrium between ocean water and the benthonic foraminifera geuns Uvigerina: Isotopic changes in the ocean during the last glacial. Colloq. Int. du Cent. Natl. la Rech. Sci. 219, 203–210 (1974).
25. Winnick, M. J. & Caves, J. K. Oxygen isotope mass-balance constraints on Pliocene sea level and East Antarctic Ice Sheet stability. Geology 43, 879–882 (2015).
26. Landais, A. et al. What drives the millennial and orbital variations of δ18Oatm? Quat. Sci. Rev. 29, 235–246 (2010).
27. Severinghaus, J. P., Beaudette, R., Headly, M. A., Taylor, K. & Brook, E. J. Oxygen-18 of O 2 Records the Impact of Abrupt Climate Change on the Terrestrial Biosphere. Science (80-.). 324, 1431–1434 (2009).
28. Bender, M., Sowers, T. & Labeyrie, L. The Dole Effect and its variations during the last 130,000 years as measured in the Vostok Ice Core. Global Biogeochem. Cycles 8, 363–376 (1994).
29. Dole, M. The relative atomic weight of oxygen in water and in air. J. Am. Chem. Soc. 57, 2731–2731 (1935).
30. Ahn, S., Khider, D., Lisiecki, L. E. & Lawrence, C. E. A probabilistic Pliocene–Pleistocene stack of benthic δ18O using a profile hidden Markov model. Dyn. Stat. Clim. Syst. 2, (2017).
31. Kuhl, T. W. et al. A new large-diameter ice-core drill: the Blue Ice Drill. Ann. Glaciol. 55, 1–6 (2014).
32. Higgins, J. A. et al. Atmospheric composition 1 million years ago from blue ice in the Allan Hills, Antarctica. Proc. Natl. Acad. Sci. 112, 6887–6891 (2015).
33. Seltzer, A. M. & Bekaert, D. V. A unified method for measuring noble gas isotope ratios in air, water, and volcanic gases via dynamic mass spectrometry. Int. J. Mass Spectrom. 478, 116873 (2022).
34. Schwander, J. The transformation of snow to ice and the occlusion of gases. in The Environmental Record in Glaciers and Ice Sheets (eds. Oeschger, H. & Langway, C. C.) 53–67 (Wiley, 1989).
35. Craig, H., Horibe, Y. & Sowers, T. Gravitational separation of gases and isotopes in polar ice caps. Science (80-.). 242, 1675–1678 (1988).
36. Sowers, T., Bender, M. & Raynaud, D. Elemental and isotopic composition of occluded O2 and N2 in polar ice. Journal of Geophysical Research, vol. 94 (1989).
37. Bereiter, B., Shackleton, S., Baggenstos, D., Kawamura, K. & Severinghaus, J. Mean global ocean temperatures during the last glacial transition. Nature 553, 39–44 (2018).
38. Jenkins, W. J., Lott, D. E. & Cahill, K. L. A determination of atmospheric helium, neon, argon, krypton, and xenon solubility concentrations in water and seawater. Mar. Chem. 211, 94–107 (2019).
39. Lambeck, K., Rouby, H., Purcell, A., Sun, Y. & Sambridge, M. Sea level and global ice volumes from the Last Glacial Maximum to the Holocene. Proc. Natl. Acad. Sci. 111, 15296–15303 (2014).
40. Seltzer, A. M., Davidson, P. W., Shackleton, S. A., Nicholson, D. P. & Khatiwala, S. Global Ocean Cooling of 2.3°C During the Last Glacial Maximum. Geophys. Res. Lett. 51, (2024).

41. Cutler, K. B. et al. Rapid sea-level fall and deep-ocean temperature change since the last interglacial period. Earth Planet. Sci. Lett. 206, 253–271 (2003).
42. Charette, M. & Smith, W. The Volume of Earth's Ocean. Oceanography 23, 112–114 (2010).
43. Raymo, M. E., Kozdon, R., Evans, D., Lisiecki, L. & Ford, H. L. The accuracy of mid-Pliocene δ18O-based ice volume and sea level reconstructions. Earth-Science Rev. 177, 291–302 (2018).

Figures

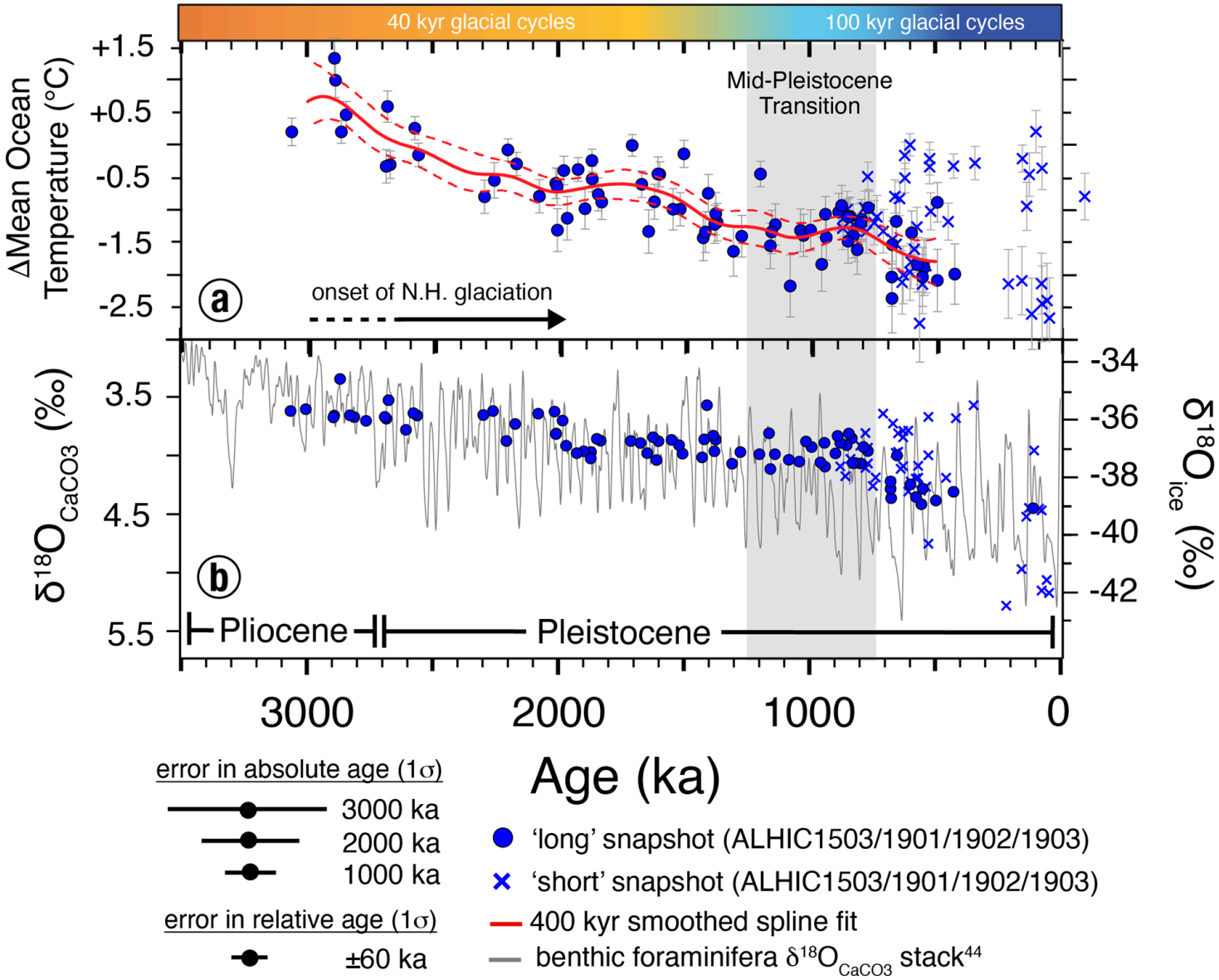

Figure 1

3 million years of mean ocean temperature from ice core noble gases. Points shown are from stratigraphically disturbed ice cores from the Allan Hills BIA dated with argon isotope ratios[12]. Samples from ALHIC1903, which is a core that is in stratigraphic order and covers Termination II[REF], is included for comparison. Error bars indicate the relative error in MOT. Points shown as 'o' indicate samples that

are characterized as ‘long exposure’ snapshots, while those shown as ‘x’ are characterized as ‘short exposure’ snapshots. Cubic spline of the record with the 1σ confidence envelope is also shown with solid line and dotted line, respectively. Data in Table S1.

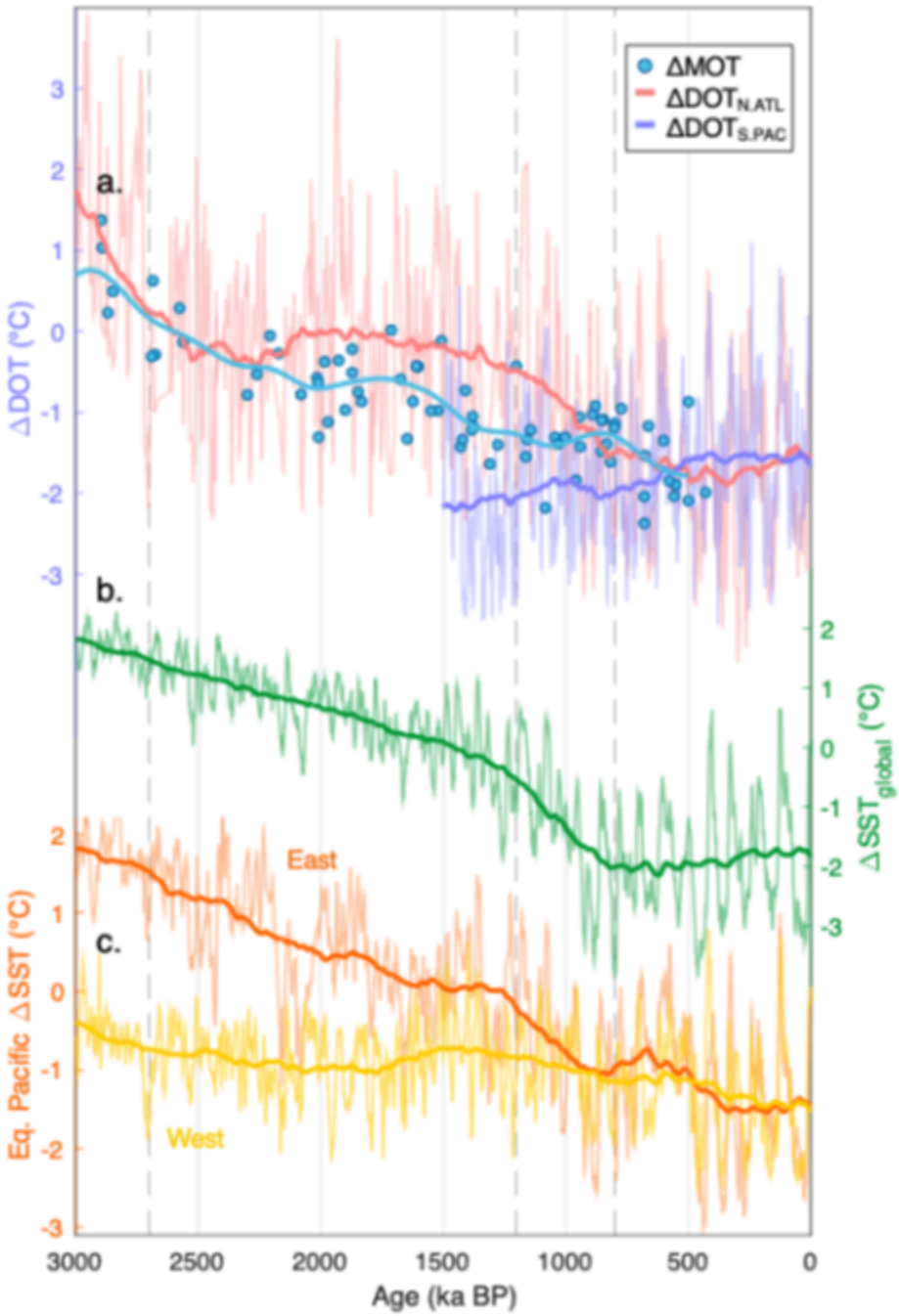

Figure 2

Surface and interior ocean temperature evolution over the last 3 million years. a) Deep ocean temperature anomalies (relative to a Holocene average) are shown for the North Atlantic[15] (pink) and South Pacific[17] (lilac). Mean ocean temperature is shown for comparison in blue. b) Global and c) equatorial Pacific sea surface temperature anomalies (relative to a Holocene average) are shown from a recent compilation[18]. In c) the orange line shows the temperature anomaly for the eastern tropical

Pacific, and the yellow line shows the Indo-Pacific warm pool. For all sediment records, the lighter colored records show the published data, and thicker and darker lines show the long-term trends from a 400kyr moving mean of the original data. For the MOT record, individual ‘long-exposure’ snapshots are shown as points and a 400-kyr moving mean of the interpolated record is shown for comparison of the long-term sediment record trends.

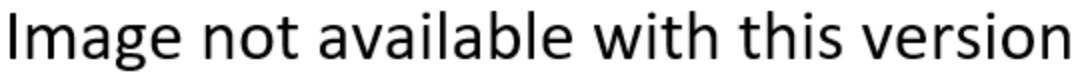

Figure 3

This image is not available with this version.

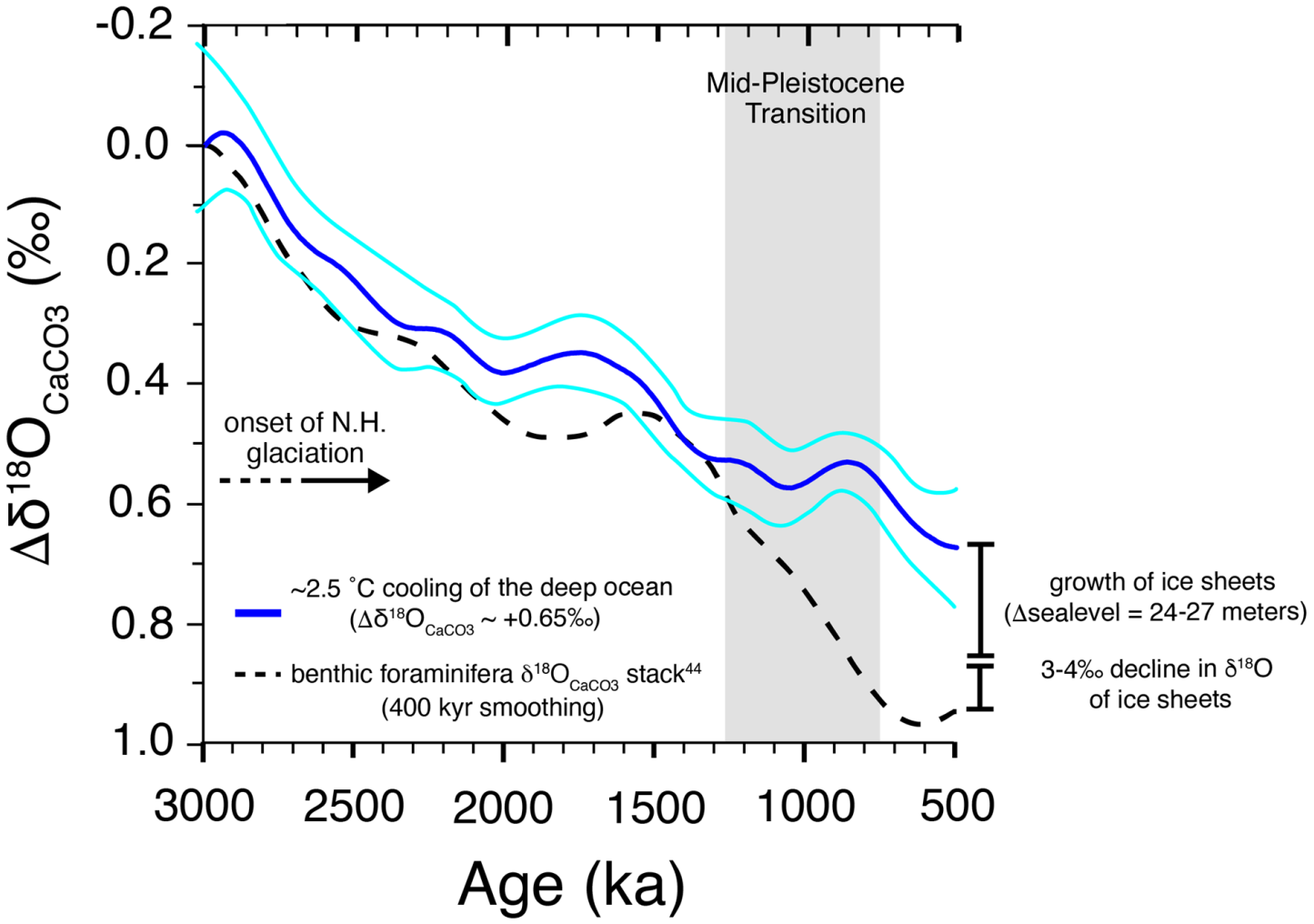

Figure 4

Contributions of temperature and ice volume to the $\delta^{18}O$ values of benthic foraminifera over the last 2.7 million years. Using our noble gas based mean ocean temperature (MOT) reconstruction and the paleotemperature equation of [24] we estimate that the $d^{18}O$ of seawater was 0.28‰ higher at 3.0 Ma compared to 0.5 Ma. This increase is very similar to that observed in the $d^{18}O_{atm}$ of 'long' snapshots from ALHIC ice cores (see text).

Supplementary Files

This is a list of supplementary files associated with this preprint. Click to download.

- SSMOTTableS1.xlsx
- SSMOTSupp.docx